

Toward Lateral Aerial Grasping & Manipulation Using Scalable Suction

Chad C. Kessens^{1,2,4,5}, Matthew Horowitz³, Chao Liu², James Dotterweich¹, Mark Yim², & Harris L. Edge¹

Abstract—This paper is an initial step toward the realization of an aerial robot that can perform lateral physical work, such as drilling a hole or fastening a screw in a wall. Aerial robots are capable of high maneuverability and can provide access to locations that would be difficult or impossible for ground-based robots to reach. However, to fully utilize this mobility, systems would ideally be able to perform functional work in those locations, requiring the ability to exert lateral forces. To substantially improve a hovering vehicle’s ability to stably deliver large lateral forces, we propose the use of a versatile suction-based gripper that can establish pulling contact on featureless surfaces. Such contact enables access to environmental forces that can be used to further stabilize the vehicle and also increase the lateral force delivered to the surface through a possible secondary mechanism. This paper introduces the concept, describes the design of a new self-sealing suction cup based on a previous design, details the design of a gripper using those cups, and describes the arm and flight vehicle. It then evaluates the cup and gripper performance in several ways, culminating in physical grasping demonstrations using the arm and gripper, including one in the presence of simulated flight noise based on data from preliminary indoor flight experiments.

I. INTRODUCTION

As the population of the world continues to move toward ever more urban areas, tall buildings with difficult-to-reach exteriors proliferate. These structures significantly increase the space that can be classified as “super-surface”, where useful work such as construction, cleaning, physical inspection, and maintenance might be necessary, but performing the work might be quite difficult, expensive, and/or dangerous due to its location. Robots that can operate in these locations present an opportunity to mitigate cost and risk, and have been successfully deployed for tasks such as installing glass ceilings [1] and cleaning [2], [3]. However, these solutions continue to require ground-based infrastructure and are specifically tailored to certain types of materials and geometries, limiting the scope of their potential use.

Aerial robots, however, are capable of reaching more generalized locations in 3D space with relative ease. The challenge is two-fold: 1) being capable of the precision necessary to perform the work and 2) delivering large enough forces, particularly laterally (i.e. perpendicular to gravity vector). First, whereas aerial robots have been performing surveillance activities for a long time [4], [5], maintaining a position and attitude while flying near clutter is particularly

difficult [6] due to the non-uniform flow of air in the presence of disturbances [7]. However, the performance of work under the vehicle has been shown in cases such as grasping in hover [8], [9] and cooperative manipulation of a rod [10].

To improve flight stability, some work has been done in utilizing environmental forces from contact [11]. This has been extended to forms of hybrid locomotion such as brachiation between flight phases [12] and spiderman-style swinging [13], but the more straightforward approach is to simply employ versatile perching on structures such as walls [14], ceilings [13], or other inclined planes [15].

The second challenge is to deliver large forces laterally. While the deliverance of stable force to a wall from an aerial vehicle has been achieved [16], [17], the magnitude of that force was modest. The problem is that an aerial vehicle uses most of its power to simply stay aloft, so it cannot deliver large lateral forces very effectively. In particular, the attitude of a traditional quadrotor is coupled with its thrust vector, and increasing lateral force delivery requires larger pitch angles, reducing the already limited vertical thrust component opposing gravity. We address these challenges using two strategies: 1) by utilizing vectored thrust [18], [19] on the aerial vehicle to decouple its attitude from force delivery and 2) by leveraging environmental forces, not just vehicle thrust, to mitigate disturbance forces and increase lateral work force capacity.

While other efforts are actively pursuing the goal of performing aerial work using traditional grippers on multi-degree of freedom arms [20], we believe that the ability to grasp and brace against featureless surfaces such as walls will bring significant versatility to the urban super-surface problem space. However, special techniques must be employed due to the need for access to local pulling forces, where traditional grippers can only push with a given contact point. One technique is to use ingressive structures such as hooks [21] or micro-spines, but these are limited to materials into which the hooks can penetrate and potentially damage the surface. Another is to use magnets [13], but again, these techniques can only grasp metal. A third technique is to use directional/reversible adhesives based on gecko setae [15], [22], [23], but these so far require clean, smooth surfaces. Finally, suction can establish these forces [14], but requires non-porous regions beneath the cups, and the more robust use of active suction [24] tends to scale poorly by requiring active valve management.

In this paper, we propose the use of an active suction gripper based on our patented self-sealing suction technology [25], which makes suction-based surface adhesion easily

¹Army Research Laboratory, Aberdeen Proving Ground, MD 21005

²GRASP Laboratory, University of Pennsylvania, Philadelphia, PA 18972

³Engility Corporation, Aberdeen Proving Ground, MD 21005

⁴Dept. of Mech. Eng., Univ. of Maryland, College Park, MD 20740

⁵Email: chad.c.kessens.civ@mail.mil



Fig. 1. Urban settings are rife with featureless surfaces such as glass and metal that could potentially be used as lateral grasp locations for a suction-based gripper, enabling the leveraging of large environmental forces.

scalable. That gripper would be mounted on a lightweight, compact Spiral Zipper arm [26], and flown on a eight-rotor propulsion core utilizing thrust vectoring of each propeller, as shown in Fig. 1, with the intent of performing aerial work such as sensor delivery to a wall, physical inspection, or even drilling a hole. The gripper’s ability to grasp featureless surfaces in a versatile way grants the vehicle access to environmental forces and torques that can be used for position stabilization, perching, and force delivery through a potential secondary mechanism. Here, we take the first step toward realizing the full system. We begin by describing a new version of a previously introduced self-sealing suction cup [25], to which significant changes have been made for increasing its scale. We then describe the components of the system, namely the gripper, zipper arm, and propulsion core. Next, we test the force required to activate the cup, its ability to resist normal forces, and its response to angular misalignment and ability to grasp cylinders. Finally, we integrate the gripper and arm onto an air frame and demonstrate wall grasping in the presence of positional noise by simulating experimental flight data from the aerial platform.

II. DESIGN

A. New Self-Sealing Suction Cup

We propose to use active suction in order to fully utilize all available wrenches on featureless surfaces. To easily maximize scalability and versatility of active suction systems, we previously introduced the concept of a self-sealing suction cup [25]. This technology features an internal valve such that the cup remains sealed when not engaged in object contact. However, a small force against the cup lip actuates an internal lever that lifts and compresses the internal plug, opening the valve and allowing the air inside the cup to be evacuated. Such a technology allows for simple, but scalable suction, where all cups can be connected to one central vacuum source, but any subset of the cups may be used without computation or active sensing to determine how to actuate the system, saving power and complexity.

For this paper, we seek significantly greater forces than our previous cup version [9] could achieve. However, scaling the design caused the structures of the cup to fail long before the

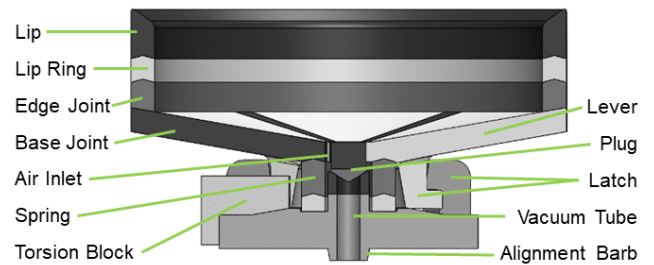


Fig. 2. Cross-sectional image of the new larger self-sealing cup design (prongs not shown). Black parts are rubber; white parts are plastic.

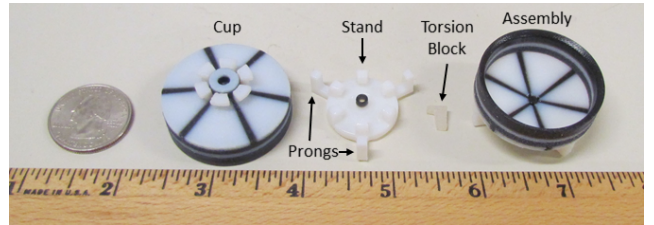


Fig. 3. Manufactured large self-sealing suction cup parts: US quarter (for size comparison), upside down cup part, stand with inlet, torsion block, fully assembled cup.

cup would otherwise forcibly disengage. Therefore, we have significantly modified the design to support this size increase. Fig. 2 shows a cross-sectional view of the new design. First, we significantly reduced the amount of rubber in the base of the cup to limit inward bulging stresses when evacuated. Second, we introduced prongs to prevent large compressive loads from breaking the cup. However, the most significant change was to introduce a latching mechanism beneath the cup. This prevents damage to the sensitive internal spring when the cup is under shear or tensile loads. Instead, those forces are passed through the plastic latch structure. Finally, a torsion block is glued between the latches to prevent twisting of the spring. Fig. 3 shows a fully assembled cup and its manufactured components.

B. Suction-based Gripper

Having developed the larger version of the self-sealing suction cup, we desired the ability of the final vehicle to perch on the underside of a ceiling. In addition, we wanted the ability to grasp not just walls, but other objects of interest such as an I-beam, light fixture, or pole, even down to a small object such as a cell phone. Therefore, our design requirements suggested multiple cups capable of handling a total load of up to 15 kg (our initial estimated total vehicle weight) with a safety factor S_f of 2 times the theoretical max load. Considering the maximum load equation

$$L_{max} = \frac{nP(\pi r^2)}{S_f} \quad (1)$$

where n is the number of cups, r is the radius of each cup (assuming they are all the same), and P is the expected pressure differential, we determined that five cups with radius $r = 16.5$ mm would appropriately support the vehicle weight,

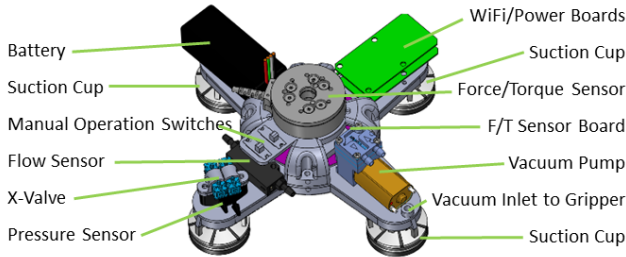


Fig. 4. Schematic of the suction-based gripper.

assuming our pump could provide at least 70 kPa pressure differential.

This pressure differential was achievable using a 55 gram CTS diaphragm micro-pump from Parker, and we used an MPX5500 pressure sensor from Freescale to maintain awareness of the internal pressure state. To switch between grasp and release modes, we plumbed in a miniature pneumatic solenoid X-valve by Parker. Finally, we wanted to provide information regarding the force and torque at the wrist, so we used a 6-axis Mini-45 force torque sensor from ATI. The information from each sensor was output wirelessly using a Sparkfun microboard, and providing the hand with its own battery made the system completely modular. The five cups were arranged in a plus shape, equally spaced 76 mm apart (center to center), with the electronic components attached to the back-side as shown in Fig. 4. In addition, to provide a mechanical capacitance that would decrease cup evacuation time while also reducing mass, the inside of the gripper body was hollowed out. The gripper body was produced on an Eden260 3D printer using VeroGray material, and the overall mass of the hand including all components was 589 g, driven largely by the force sensor.

C. Spiral Zipper Arm

The gripper is attached to a Spiral Zipper arm [26], a robot manipulator with Cartesian coordinate control (x, y, z) using three tethers and one Spiral Zipper tube. We developed two type of modules — tether modules and tube modules — to construct the robot. The tethers and Spiral Zipper tube, while very light, are powerful enough to maintain heavy loads as desired. A simple spool attached to the motor shaft is used to drive the tether, and an omni-wheel driving mechanism, shown in Fig. 5, is designed to drive the Spiral Zipper tube in and out.

All three tether links and one tube link are joined together at the end of the Spiral Zipper tube where the gripper is attached, as shown in Fig. 6. The state of the arm is modeled as a 3D vector denoting the position of the gripper, and a nested position controller controls the motion of the gripper.

D. Propulsion Core

The arm and gripper will be attached to a uniquely designed Unmanned Aerial System (UAS) we call a propulsion core. In the instantiation used for this paper, it has eight reconfigurable propeller pods, each capable of thrust

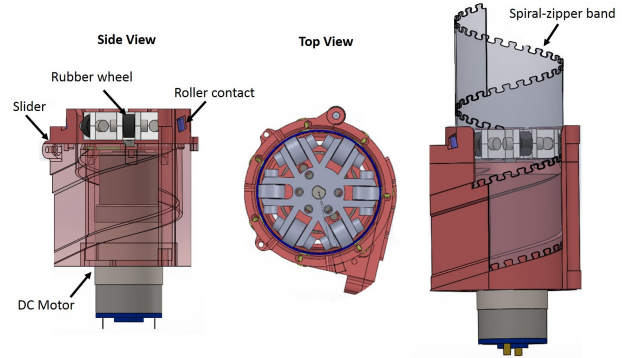


Fig. 5. Spiral Zipper driving mechanism using omni-wheel. Rollers on the omni-wheel allow band to extend or retract as the system rotates.

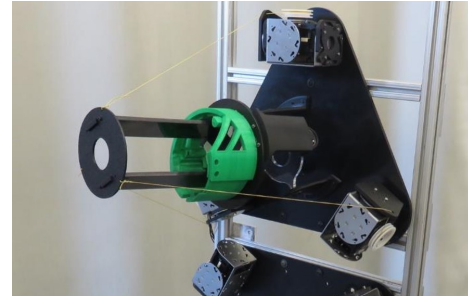


Fig. 6. Physically manufactured Spiral Zipper arm.

vectoring about a single axis, and all mounted in an enclosed carbon fiber tube frame. Fig. 7 shows the physically realized propulsion core. Here, the frame itself is built to be strong and rigid, yet lightweight both to protect the propellers from striking the environment but also to be able to impact surfaces for force transmission. The pods are all mounted to vector along the pitch axis, allowing the vehicle to pitch in place without changing position, unlike a conventional thrust-based vehicles such as a quadrotor. This increases the effective workspace of any robotic limb mounted to the propulsion core, in this case the Spiral Zipper arm. The propulsion core flight system uses a Pixhawk flight controller running a modified PX4 v1.6.5 flight stack as the base autopilot, with an Odroid XU4 running custom software for coordinated vehicle and arm controls in a Linux environment. Each thrust vectoring pod consists of a U7 490kV T-motor with a 40.6 cm carbon fiber prop and a MX-28 Dynamixel servo for rotation. The vehicle dimensions are 0.93 x 1.85 x 0.66 meters, with a total vehicle mass of 13 kg. The lift capacity is approximately 400 N, giving a thrust to weight ratio of 3:1. The flight time is approximately 15 min on two 22.2 V 10900 mAh Lipo battery packs, wired such that each pack powers a set of four motors.

III. GRIPPER TESTING AND RESULTS

A. Cup Normal Force

To characterize the performance of the gripper, we began by testing the response of the suction cup to normal force. First, we fixed a single cup to the bottom of an Instron 5965

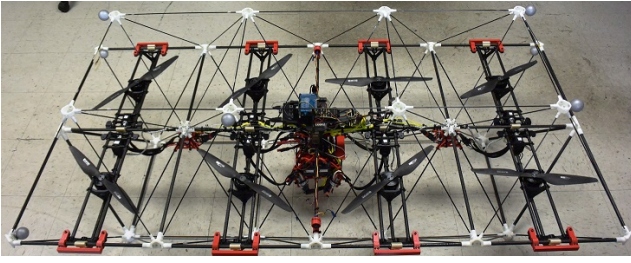


Fig. 7. Propulsion Core hardware platform.

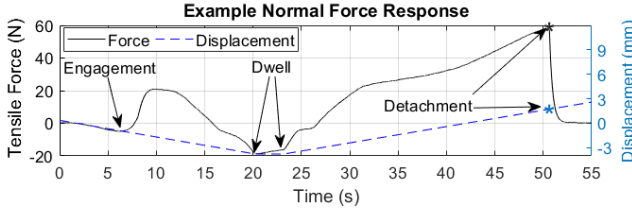


Fig. 8. Example normal force response of cup (black) to object displacement (blue) relative to initial cup contact plane. Object velocity was 0.2 mm/s down and up, with a 3 s dwell at the lowest position. Force was measured using a Mini-45 force-torque sensor from ATI.

Universal Testing System and drew a vacuum using the CTS micro-diaphragm pump on the gripper. We then affixed a flat plate to the top of the machine with a Mini-45 force torque sensor from ATI in between. Next, the top plate was lowered at a rate of 0.2 mm/s until the compressive force reached 20 N. After dwelling there for 3 s, the top plate was raised at a rate of 0.2 mm/s until the cup forcibly detached from the top plate.

Fig. 8 shows an example normal force response as a function of time. As the plate is lowered, the compressive force (negative tensile force) increases until a threshold force is overcome, opening the cup’s internal valve. The force on the object then rapidly switches from compressive to tensile as the air in the cup is evacuated and suction is engaged. Once the bottom position is reached, the viscoelastic properties of the rubber material cause some relaxation during the dwell. Upon rising, the internal stresses on the cup create a non-linear force response due to the changing mix of plastic-on-plastic contact and deformation of various rubber parts. Finally, a peak holding threshold is reached where the object is forcibly detached from the object. Detachment occurred 1.8 mm above the nominal lip plane of the cup. Over five tests, release forces averaged 57.2 ± 10.2 N, and threshold forces averaged 4.6 ± 1.7 N. We are as yet unsure of the reason for the large deviation in release force.

B. Planar Misalignment

Next, we sought to determine the cup’s ability to accommodate angular misalignment. The natural compliance in the cup should allow it to successfully engage, even if not perfectly aligned. To test this, we created planar objects varying in 3 degree increments and tested the threshold force required to activate the cup as well as the holding force. These angled planar objects were attached to the top of the

Instron in place of the original object, and the procedure described in section III-A was repeated. Note: if attachment was not achieved, the compressive force setpoint at which the Instron was programmed to stop lowering was increased to create the attachment.

At a 3 degree offset, the response was indistinguishable from the aligned plane, with a threshold force of 3.3 N and a maximum holding force of 62.9 N, both within the expected margin of error. At a 6 degree angular misalignment, the cups were still able to engage, but required a mean threshold force of 31.8 N, and could only resist a mean force of 25.3 N. At 9 degrees, the cups were no longer able to engage the plane using a reasonable compressive force.

C. Cup Performance on Cylindrical Objects

Beyond planar objects, super-surface environments also tend to be rich with cylindrical objects such as pipes and poles. Thus, we sought to test the cup’s ability to grasp cylindrical objects. However, cylinders present a particular challenge because the planar contact surface of the cup lip does not match the orthogonally circular surface of the cylinder. To attach, internal stresses within the lip must be developed at the cost of reducing the cup’s ability to maintain its grasp on the cylinder. In addition, more force would be required to engage the cup due to the additional penetration depth along the center of the lip that is necessary to allow the outer edges of the cup to contact the cylinder.

To test these effects, we 3D printed cylindrical objects of varying radii out of VeroWhite using an Objet Eden 260. The radii were chosen as a function of the percentage of the cup lip the cylinder would need to penetrate before the outer edge of the lip contacted the cylinder. The following equation was derived and used:

$$R_{cyl} = \frac{(\epsilon h_{lip})^2 + r_{cup}^2}{2\epsilon h_{lip}} \quad (2)$$

where R_{cyl} is the radius of the cylinder, ϵ is the percent penetration to create full lip contact, $h_{lip} = 3.9$ mm is the total lip height, and $r_{cup} = 16.5$ mm is the radius of the cup. We then tested the cups according to the procedure described in section III-A, again varying the maximum compressive force setpoint as needed.

Fig. 9 shows the results of these experiments. As expected, the maximum holding force decreased as the radius of the cylinder decreased (corresponding to an increase in required lip compression). In addition, the compressive force required to engage the cup on the cylinder also increased (larger negative magnitude in the figure), requiring 56.3 N of force to engage a cylinder with a radius of 88.0 mm. The cup was unable to grasp the next size smaller cylinder.

D. Static Grasping

Finally, we sought to demonstrate that the gripper was capable of holding an object approximately equivalent in mass to that of the flight vehicle. Fig. 10 shows the gripper easily grasping a 15 kg slab of polycarbonate, suggesting that it should similarly support the vehicle perched on the

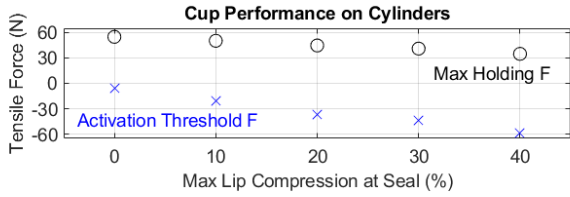


Fig. 9. Maximum holding force and activation threshold force for new large cup on cylindrical objects with varying radius. Radii chosen as a function of the theoretical percentage of lip penetration required to create a seal ($r = \infty$, 349, 175, 117, and 88 mm, left to right)



Fig. 10. Gripper grasping a) 15 kg slab of polycarbonate and b) 1.1 kg plastic bucket ($r = 13.8$ cm at center).

underside of a ceiling, for example. A single cup grasping a 1.1 kg plastic bucket with 138 mm radius is also shown.

IV. VEHICLE TESTING AND RESULTS

A. Flight Noise Estimation

Having performed a preliminary evaluation of the gripper, we next sought to demonstrate the possibility of grasping from the vehicle. The challenge is that the aerial vehicle is subject to position and attitude noise as a function of the environmental conditions and the performance of the controller onboard. While we are actively working to improve this controller, we obtained test data for the vehicle using the PixHawk flying in a quadrotor-like format (without vectoring) to establish a baseline noise level and determine if the gripper could successfully attach under those conditions. Our expected operational procedure for attachment is to extend the arm such that the flight vehicle can attach to the wall before it begins to experience wall effects that might provide additional challenges to the controller. Therefore, we obtained test data from a 90 s flight without obstacle interference, where the vehicle was attempting to maintain its position and attitude in position hold mode using Vicon motion capture positions well above ground effect.

Fig. 11 shows a plot of the x and y position of the vehicle during the test flight. In the x direction (long axis of vehicle), the vehicle maintained its position within a maximum range of ± 13 cm with a standard deviation of 6 cm at a frequency of 0.33 Hz. In the y direction, the vehicle maintained its position within a maximum range of ± 26 cm with a standard deviation of 8 cm at a frequency of 0.22 Hz based on the principal component of the FFT analysis.

Fig. 12 shows a plot of the vehicle's yaw and pitch angles as a function of time. Here, the vehicle maintained its yaw attitude within a range of ± 4.4 deg with a standard deviation of 1.5 deg and a frequency of 0.37 Hz. Pitch attitude was

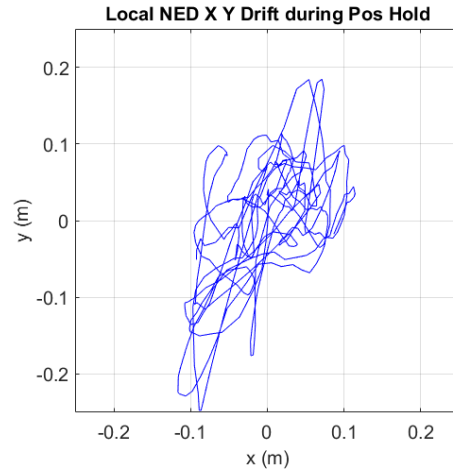


Fig. 11. X and Y position of the flight vehicle in position hold.

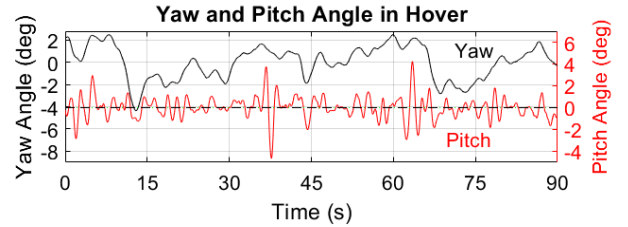


Fig. 12. Yaw angle of the flight vehicle in position hold.

maintained within a range of ± 4.7 deg with a standard deviation of 1.0 deg and a frequency of 0.45 Hz.

B. Lateral Grasping with Simulated Flight Noise

Our final test was to demonstrate lateral grasping in the presence of noise. For safety during these initial experiments, we mounted the arm and gripper on an air frame, which was then mounted to a cart with 4 caster wheels. The arm was extended toward a metal trash bin located at the edge of the vehicle's positional error bubble as defined in section IV-A. The positional and angular noise was then simulated by moving the cart within the bounds of the data bubble at the appropriate frequencies using a metronome. As the cart moved within this noise, it grasped the trash bin and maintained the grasp exerting a peak force of 19.8 N, demonstrated in the video included with this submission. The grasp released under a moment of 0.89 Nm. In a separate experiment without vehicular noise, we also demonstrated grasping the bin via arm extension and then pulled the vehicle toward the bin.

V. CONCLUSIONS AND FUTURE WORK

In this paper, we detailed the design of a new manipulation system for aerial systems to perform work with large lateral forces. This included a gripper based on a new self-sealing suction cup, a spiral zipper arm, and an eight rotor propulsion core. We then characterized the cup's response to normal forces and its ability to grasp angled surfaces and cylinders of varying radius. Finally, we demonstrated grasping of a

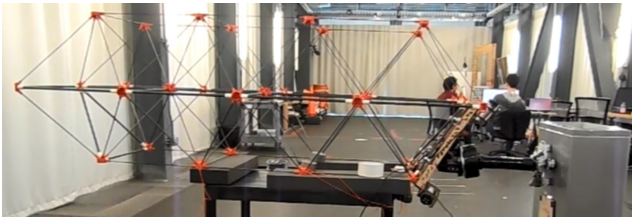


Fig. 13. Arm and gripper on a propulsion core frame mounted to a cart. Vertical metal surface (trash bin) was grasped in the presence of simulated positional noise.

vertical plane in the presence of simulated flight noise based on experimental flight data, as well as the vehicle's ability to pull itself toward the plane once grasped.

In future work, we intend to improve the vehicle flight controller, particularly for flight in the presence of obstacles, and couple control of the configurable vehicle attitude dynamics of the propulsion core with the limb dynamics to increase effectiveness. We also plan to relocate flight hardware (e.g. batteries) onboard the propulsion core to balance the moment induced by the additional mass of the manipulator. Finally, we intend to improve the robustness of the arm and hand, improve torque resistance, demonstrate lateral aerial grasping from the flying vehicle, and add a second mechanism through which we can accurately transmit large lateral loads for performing meaningful work.

ACKNOWLEDGMENTS

The authors express their sincerest thanks to Albert Tran of Engility Corporation for his assistance using equipment to gather cup performance data, as well as to Yiming Zhang and Xiaoshan Lin at the University of Pennsylvania for assistance with the hardware demonstrations.

This work was conducted in part through collaborative participation in the Robotics Consortium sponsored by the U.S Army Research Laboratory under the Collaborative Technology Alliance Program, Cooperative Agreement W911NF-10-2-0016. The views and conclusions contained in this document are those of the authors and should not be interpreted as representing the official policies, either expressed or implied, of the Army Research Laboratory of the U.S. Government. The U.S. Government is authorized to reproduce and distribute reprints for Government purposes notwithstanding any copyright notation herein.

REFERENCES

- [1] S. Lee, M. Gil, K. Lee, S. Lee, and C. Han, "Design of a ceiling glass installation robot," in *Proceedings of the 24th International Symposium on Automation and Robotics in Construction*, pp. 247–252, 2007.
- [2] W. Yan, L. Shuliang, X. Dianguo, Z. Yanzheng, S. Hao, and G. Xueshan, "Development and application of wall-climbing robots," in *Robotics and Automation, 1999. Proceedings. 1999 IEEE International Conf. on*, vol. 2, pp. 1207–1212, IEEE, 1999.
- [3] H. Zhang, J. Zhang, G. Zong, W. Wang, and R. Liu, "Sky cleaner 3: A real pneumatic climbing robot for glass-wall cleaning," *IEEE Robotics & Automation Magazine*, vol. 13, no. 1, pp. 32–41, 2006.
- [4] P. Y. Oh, M. Joyce, and J. Gallagher, "Designing an aerial robot for hover-and-stare surveillance," in *Advanced Robotics, 2005. ICAR'05. Proc., 12th International Conference on*, pp. 303–308, IEEE, 2005.

- [5] M. Onosato, F. Takemura, K. Nonami, K. Kawabata, K. Miura, and H. Nakanishi, "Aerial robots for quick information gathering in usar," in *SICE-ICASE, 2006. Int'l Joint Conf.*, pp. 3435–3438, IEEE, 2006.
- [6] K. Steich, M. Kamel, P. Beardsley, M. K. Obrist, R. Siegwart, and T. Lachat, "Tree cavity inspection using aerial robots," in *2016 IEEE/RSJ International Conf. on Intelligent Robots and Systems (IROS)*, pp. 4856–4862, IEEE, 2016.
- [7] F. Santoso, M. A. Garratt, and S. G. Anavatti, "State-of-the-art intelligent flight control systems in unmanned aerial vehicles," *IEEE Trans. on Automation Sci. and Eng.*, vol. 15, no. 2, pp. 613–627, 2018.
- [8] P. E. Pounds, D. R. Bersak, and A. M. Dollar, "Practical aerial grasping of unstructured objects," in *Technologies for Practical Robot Applications (TePRA), 2011 IEEE Conf. on*, pp. 99–104, IEEE, 2011.
- [9] C. C. Kessens, J. Thomas, J. P. Desai, and V. Kumar, "Versatile aerial grasping using self-sealing suction," in *Robotics and Automation (ICRA), 2016 IEEE Int'l Conf. on*, pp. 3249–3254, IEEE, 2016.
- [10] S. Kim, H. Seo, J. Shin, and H. J. Kim, "Cooperative aerial manipulation using multirotors with multi-dof robotic arms," *IEEE/ASME Transactions on Mechatronics*, vol. 23, no. 2, pp. 702–713, 2018.
- [11] R. Naldi, A. Macchelli, N. Mimmo, and L. Marconi, "Robust control of an aerial manipulator interacting with the environment," *IFAC-PapersOnLine*, vol. 51, no. 13, pp. 537–542, 2018.
- [12] Q. Delamare, P. R. Giordano, and A. Franchi, "Toward aerial physical locomotion: The contact-fly-contact problem," *IEEE Robotics and Automation Letters*, vol. 3, no. 3, pp. 1514–1521, 2018.
- [13] K. Zhang, P. Chermprayong, T. Alhinai, R. Siddall, and M. Kovac, "Spidermav: Perching and stabilizing micro aerial vehicles with bio-inspired tensile anchoring systems," in *2017 IEEE/RSJ Int'l Conf. on Intelligent Robots and Systems (IROS)*, pp. 6849–6854, IEEE, 2017.
- [14] H. W. Wopereis, T. van der Molen, T. Post, S. Stramigioli, and M. Fumagalli, "Mechanism for perching on smooth surfaces using aerial impacts," in *Safety, Security, and Rescue Robotics (SSRR), 2016 IEEE International Symposium on*, pp. 154–159, IEEE, 2016.
- [15] J. Thomas, M. Pope, G. Loianno, E. W. Hawkes, M. A. Estrada, H. Jiang, M. R. Cutkosky, and V. Kumar, "Aggressive flight with quadrotors for perching on inclined surfaces," *Journal of Mechanisms and Robotics*, vol. 8, no. 5, p. 051007, 2016.
- [16] A. Albers, S. Trautmann, T. Howard, T. A. Nguyen, M. Frietsch, and C. Sauter, "Semi-autonomous flying robot for physical interaction with environment," in *Robotics Automation and Mechatronics (RAM), 2010 IEEE Conference on*, pp. 441–446, IEEE, 2010.
- [17] S. Hamaza, I. Georgilas, and T. Richardson, "An adaptive-compliance manipulator for contact-based aerial applications," in *2018 IEEE/ASME International Conf. on Advanced Intelligent Mechatronics (AIM)*, pp. 730–735, IEEE, 2018.
- [18] S. Khoo, M. Norton, J. J. Kumar, J. Yin, X. Yu, T. Macpherson, D. Dowling, and A. Kouzani, "Robust control of novel thrust vectored 3d printed multicopter," in *Control Conference (CCC), 2017 36th Chinese*, pp. 1270–1275, IEEE, 2017.
- [19] D. Invernizzi and M. Lovera, "Trajectory tracking control of thrust-vectoring uavs," *Automatica*, vol. 95, pp. 180–186, 2018.
- [20] A. Suarez, A. E. Jimenez-Cano, V. M. Vega, G. Heredia, A. Rodriguez-Castaño, and A. Ollero, "Design of a lightweight dual arm system for aerial manipulation," *Mechatronics*, vol. 50, pp. 30–44, 2018.
- [21] D. Mellinger, Q. Lindsey, M. Shomin, and V. Kumar, "Design, modeling, estimation and control for aerial grasping and manipulation," in *Intelligent Robots and Systems (IROS), 2011 IEEE/RSJ International Conference on*, pp. 2668–2673, IEEE, 2011.
- [22] A. Kalantari, K. Mahajan, D. Ruffatto, and M. Spenko, "Autonomous perching and take-off on vertical walls for a quadrotor micro air vehicle," in *2015 IEEE International Conf. on Robotics and Automation (ICRA)*, pp. 4669–4674, IEEE, 2015.
- [23] M. Dadkhah, Z. Zhao, N. Wettels, and M. Spenko, "A self-aligning gripper using an electrostatic/gecko-like adhesive," in *2016 IEEE/RSJ International Conf. on Intelligent Robots and Systems (IROS)*, pp. 1006–1011, IEEE, 2016.
- [24] H. Tsukagoshi, M. Watanabe, T. Hamada, D. Ashlih, and R. Iizuka, "Aerial manipulator with perching and door-opening capability," in *Robotics and Automation (ICRA), 2015 IEEE International Conference on*, pp. 4663–4668, IEEE, 2015.
- [25] J. P. Desai and C. Kessens, "System, method, and apparatus for suction gripping," Feb. 26 2013. US Patent 8,382,174.
- [26] F. Collins and M. Yim, "Design of a spherical robot arm with the spiral zipper prismatic joint," in *Robotics and Automation (ICRA), 2016 IEEE Int'l Conf. on*, pp. 2137–2143, IEEE, 2016.